Experimental Study on Sedimentation over the Floodplain due to River Embankment Failure

By Md. Zahurul ISLAM, Kenji OKUBO, Yoshio MURAMOTO and Hiroshi MORIKAWA

(Manuscript recieved on June 2, 1994, revised on September 21, 1994)

Abstract

River embankment failure and floodplain sedimentation are common and frequent natural disasters in alluvial rivers. In Bangladesh, for instance, every year hundreds of embankments are damaged by flood water resulting in crop damage due to inundation and sedimentation. To elucidate the process of sedimentation over the vegetated floodplain due to embankment failure, a basic series of laboratory experiments was carried out with different lengths of embankment breach and different heights of model plant in the floodplain. The sediment volume and thickness over the floodplain increased with the increase of the breach length in the embankment. The maximum thickness upto a definite limit attained in the early stage was almost equal to or less than the water depth in the floodplain. Sedimentation was also observed to be greater in the floodplain with the more retardative jute field than in that with the rice field. Volume and area of sedimentation increased significantly with the increase of sediment inflow into the floodplain, namely the flood duration, the discharge and sediment concentration in the river.

1. Introduction

Bangladesh is a disaster prone country where flood and river embankment failure resulting in sedimentation over the floodplain are common and frequent natural hazards. The major river system, the Ganges-Brahmaputra-Meghna and their tributaries and distributaries carry 13 millions of tons of suspended sediments per day (Coleman, 1969). Choudhury (1990) noted that about 80% of the surface flows concentrate during the monsoon (June to September) that carry about 2.4 billion tons of sediments a year through the river system of Bangladesh. These sediments settle over the river beds, floodplains and low lying areas during the inundation and with the recession of flood water. As a result river channels and their distributaries are silted up with sediments composed of fine sands and silts causing drainage congestion and overbank flow resulting in river embankment failure and sedimentation over the floodplain causing a severe damage to agricultural crops (Ahmed et al., 1992, Bangladesh Water Development Board, 1987; Hoque et al., 1991; Klaassen et al., 1988 and Pramanik, 1993).

An investigation carried out in Institute of Flood Control and Drainage Research, Bangladesh University of Engineering and Technology, showed that only ten breaches of eight embankments caused sediment deposition to amount to more than 16 million m^3

over the floodplain vegetated with young rice and jute plants causing damage to agricultural crops of about 66,700 hectares (Islam, 1991). The simply averaged thickness of the sedimentation within the flood affected areas was obtained as 2.4 cm. Meanwhile it was found from the field survey after the flood that the actual thickness of near breach deposition in the vicinity of embankment was at least ten times higher than the average. It was also noticed that the deposited material was rather silty and riverborn. Little is known, however, about the sediment inflow condition through the embankment when the breach was actively taking place. Therefore, it seemed that some basic experiments would be needed employing a physical model to observe the whole process of sedimentation over the floodplain due to river embankment failure with different breach lengths and vegetation types, by controlling flood duration, discharge and sediment concentration in the river channel.

This paper describes the results of the experiments carried out using a physical model in the hydraulic laboratory at Disaster Prevention Research Institute of Kyoto University with the following objectives:

i) To study the effects of different breach lengths in the river embankment and of different heights of vegetation on the floodplain sedimentation,
ii) To observe the whole process of floodplain sedimentation by changing the duration, discharge and sediment concentration in river channel.

This kind of study is rare in the available literature except for a few recent studies; Takahashi et al.(1988) and Muramoto et al.(1989) demonstrated overbank flows and sedimentation processes due to floods of rivers. Nakagawa et al.(1989) and Shieh (1989) described the sedimentation due to sediment laden jets entering the basins at a right-angle.

2. Experimental Set-up

The experiments were carried out by using a distorted model according to the scheme shown in **Table 1**. The plan and side views of the model are shown in **Fig. 1**. The working section connecting the up and downstream basins is 200 cm long with a constant longitudinal slope of 1/300. The model consists of the 15 cm wide river channel and the right side floodplain with a width of 60 cm. The floodplain is vegetated with the assumed rice and jute plants artificially made with thin plastic sticks with the plant heights (H_v) of 5.5 mm and 25 mm, respectively. The water depth (d_w) in the river and floodplain was kept always 3.6 cm.

Both rice and jute are common crops in Bangladesh, with both plants being about 100 times higher than the corresponding artificial materials selected for the present experiment. Thus, the vertical length scale ratio was taken as 100 and the corresponding water depth in the field is 3.6 m, which is a typical flood depth in this country. On the other hand, the horizontal length scale was based on the channel width, assuming the length ratio of 1,000. Then the corresponding width of flooded river becomes 150 m. The Froude similarity is expected for inflow discharges at breached sections, where the velocity is proportional to the square root of water depth, which reduces the velocity ratio

Table 1. Scheme of the experiments

Run	Experiment	L_b (cm)	T_e (min.)	Type of Vegetation	H_v (mm)
1	EBSR1	5	20	rice	5.5
2	EBSR2	10	20	rice	5.5
3	EBSR3	15	20	rice	5.5
4	EBSR4	20	20	rice	5.5
5	EBSJ1	5	20	jute	25
6	EBSJ2	10	20	jute	25
7	EBSJ3	15	20	jute	25
8	EBSJ4	20	20	jute	25
9	EBSJ2.TDP	10	100	jute	25
10	EBSJ3.TDP	15	100	jute	25
11	EBSR2.TD1	10	20	rice	5.5
12	EBSR2.TD2	10	40	rice	5.5
13	EBSR2.TD3	10	100	rice	5.5
14	EBSJ2.TD1	10	20	jute	25
15	EBSJ2.TD2	10	40	jute	25
16	EBSJ2.TD3	10	100	jute	25
17	EBSJ4.DD1	20	20	jute	25
18	EBSJ4.DD2	20	20	jute	25
19	EBSJ4.DD3	20	20	jute	25

EBSR: **E**mbankment **B**reach resulting in **S**edimentation over **R**ice field.
EBSJ: **E**mbankment **B**reach resulting in **S**edimentation over **J**ute field.
TDP: **T**ime **D**ependent, **P**reliminary Experiment.
TD: **T**ime **D**ependent Experiment.
DD: **D**ischarge **D**ependent Experiment.

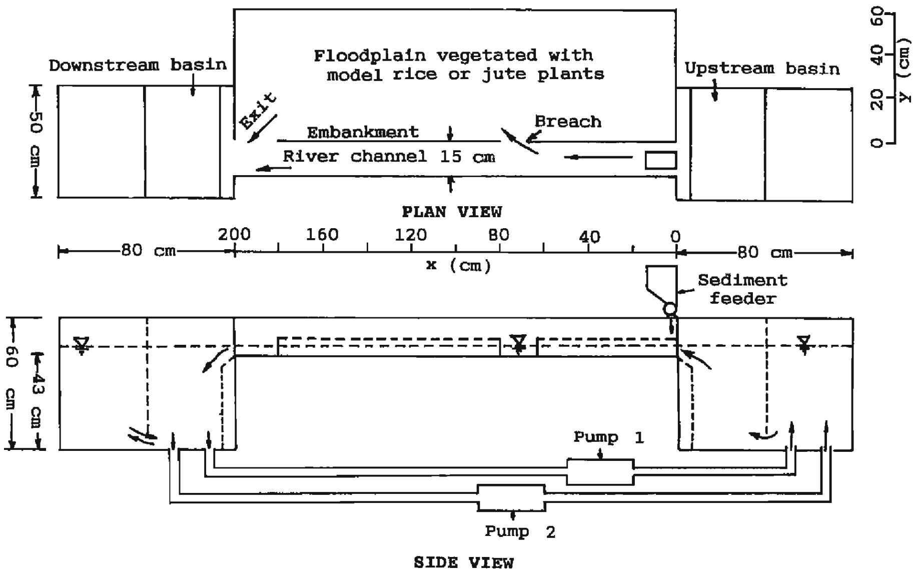

Fig. 1. Experimental set-up for sedimentation over the floodplain due to embankment failure.

of 10 and the advective time and discharge ratios become 100 and 10^6, respectively.

The model embankment was constructed by plastic plates with 7 mm in thickness, dividing the floodplain and the river channel with breach lengths (L_b) of 5, 10, 15, and 20 cm and with an exit of 20 cm at the downstream of the embankment to deliver water from the floodplain into the channel. Total discharge at the upstream section of river channel for the experiments of EBSR and EBSJ in runs 1–8 was 2,160 cm^3/s, and the sectional mean velocity was 40 cm/s. Discharge into the river channel was kept constant, while the net discharge onto the floodplain through the embankment breach increased as the breach length increased.

The downstream ends of the breaches in the embankment were fixed at $x=80$ cm. Before the commencement of the experiments, water was supplied at the up and downstream basins of the model until the attainment of 3.6 cm in depth on the floodplain as well as in the river channel. A steady state was formed in both the floodplain and river channel when the pumps were started for recycling of water in the model. Constant sediment supply at the upper end of the river channel was ensured with the help of a sediment feeder. Sediment mixers were used to mix the sediments and water in both the up and downstream basins. Turbidity meter (Model PC106, Tokyo Keisoku Co. Ltd.) was fixed at the upstream end of the river channel to obtain the record of sediment concentration in the river water. Average sediment concentration was 9,400 mg/l for all of the EBSR and EBSJ experiments and 12,000 mg/l for the time dependent experiments (EBSJ2.TDP, EBSJ3.TDP, EBSR2.TD and EBSJ2.TD in runs 9–16), while that for the discharge dependent experiments, EBSJ4.DD in runs 17–19, was kept 11,200 mg/l. **Fig. 2** shows the grain size distribution of the used sediment materials with the medium diameter of about 100 micra.

After the former part of the experiment with the elapsed time (T_e) of 20 minutes, the experiment was carried out for an additional 60 minutes following the same pro-

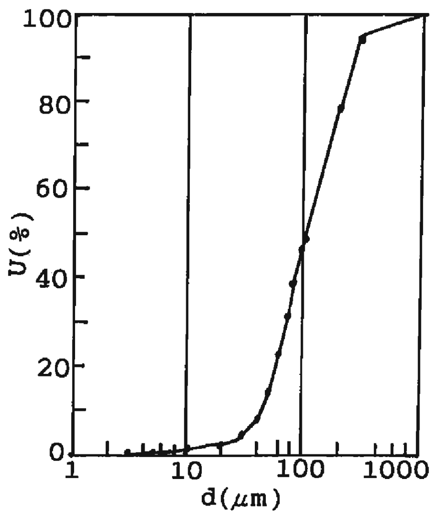

Fig. 2. Grain size distribution curve of the sediment materials.

cedure in runs 1–8. To check the results of the earlier runs, the time dependent (TD) experiments, EBSJ2.TDP and EBSJ3.TDP with the embankment breach length of 10 cm and 15 cm, respectively, were carried out with the duration of 100 minutes in runs 9–10, and the experiments of EBSR2.TD1–3 and EBSJ2.TD1–3 with the embankment breach length of 10 cm were carried out for durations of 20, 40 and 100 minutes in runs 11–16. For the discharge dependent (DD) experiments of EBSJ4.DD in runs 17–19, varying discharges of 1,080 cm^3/s, 1,620 cm^3/s and 2,160 cm^3/s were supplied in the river channel.

Measurement of sediment thickness for all the experiments was made laterally and longitudinally after every two centimeters at the points of sediment deposition over the floodplain vegetated with a model rice or jute field. It was done using a point gauge and later with the help of the laser beam gauge as a displacement sensor (Model LB10 and the amplifier Model LB60, Keyence). The thickness was measured from the base level of the vegetated floodplain. Reduction in total deposited volume due to the plants was taken into account for later discussion, which were approximated by uniform fractions of 4% for the rice plant and 12% for the jute plant to the total volumes. For determination of length (L_s) and width (W_s) of scour holes that formed immediately beyond the breach, several measurements were taken longitudinally and laterally, and the average length and width of the scour holes were obtained.

3. Sedimentation Patterns over the Floodplain

3.1 Sedimetation patterns affected by vegetation

Sedimentation views and their patterns over the floodplain in EBSR and EBSJ are shown in **Photos 1** and **2**, and **Figs. 3** and **4**, respectively. It is seen from the photos and figures that both the area and volume of sedimentation increased when the breach length was increased as 5, 10, 15, and up to 20 cm. Similar sediment deposition for EBSR and EBSJ was observed to be higher in EBSJ than in EBSR.

In EBSR, the sediment distribution patterns were observed to be longer in shape over the floodplain along the flow axis of the sediment laden jet through the breaches forming long scouring holes immediately beyond the breaches in the land-side. The deposition was closer to the model boundary wall opposite to the embankment across the floodplain. In **Photo 1**, the sediment deposition looks wavy and covered with ripples and holes formed over the deposited area. As the sedimentation increased, rice plants became less visible losing their roughness effect. In the midstream of the floodplain, sediment transport lasted, and turbid water came out at the exit of the floodplain.

In EBSJ, in contrast, the main part of the sediment deposition over the vegetation was delineated by a sharp edge beyond which the deposition height rapidly decreased, and was found to be almost smooth and flat without any ripple formed, over which a shallow flow of water was observed. The shapes were almost round forming very minor scouring holes just beyond the breach in the land-side. But the smooth, flat surface of the main deposition would sometimes be disturbed by fine scale channel formation at later stages. Particles were trapped on the outer slope of the main deposition, so that

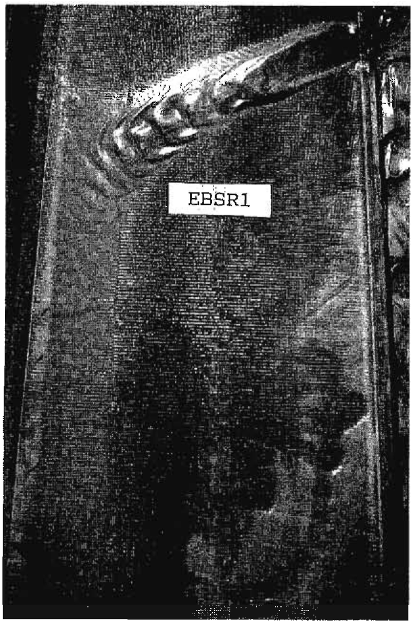

a) EBSR1 : 5 cm

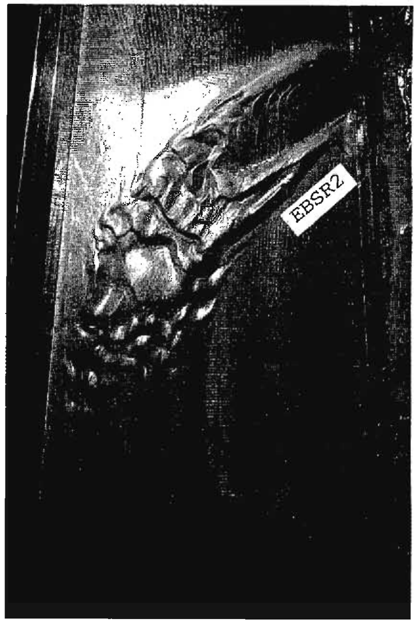

b) EBSR2 : 10 cm

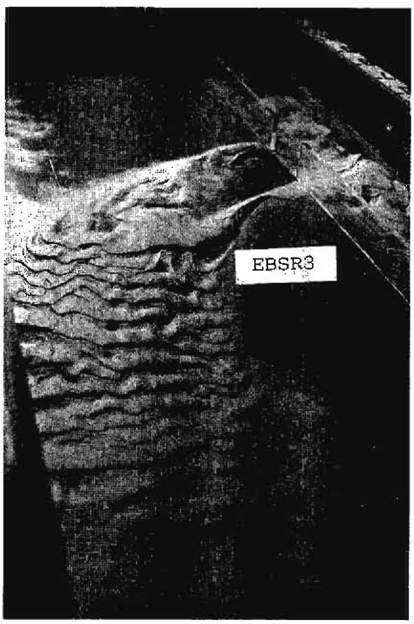

c) EBSR3 : 15 cm

d) EBSR4 : 20 cm

Photo 1. Sediment distribution over the floodplain vegetated with model rice plants in the exp. EBSR.

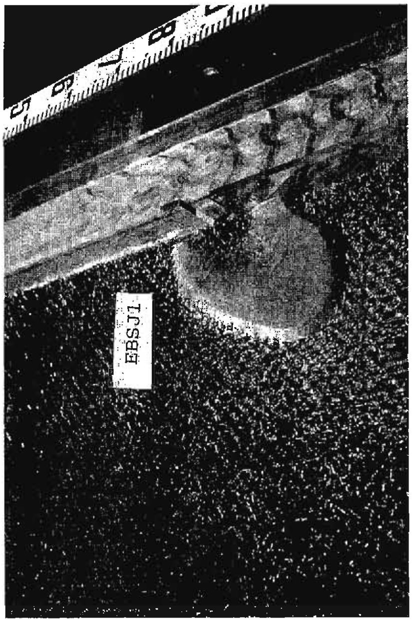

a) EBSJ1 : 5 cm

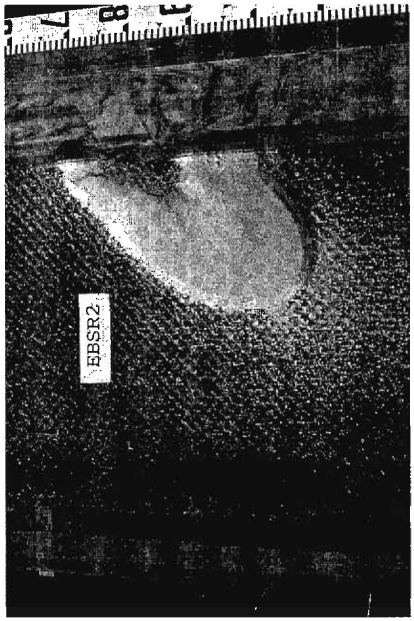

b) EBSJ2 : 10 cm

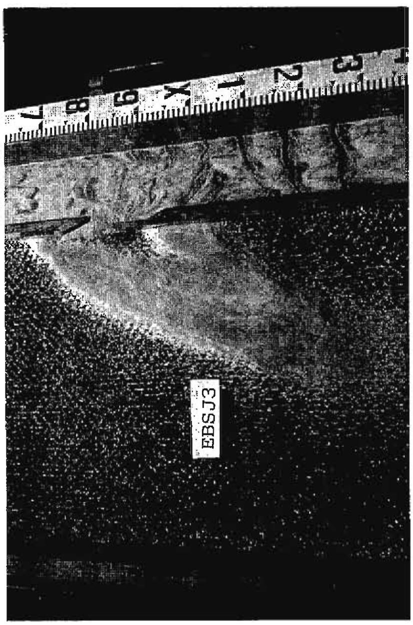

c) EBSJ3 : 15 cm

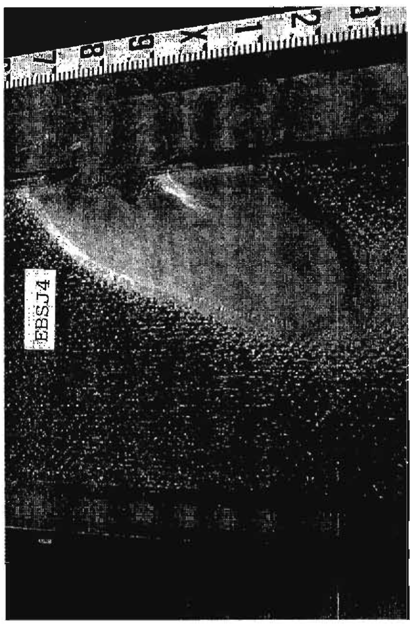

d) EBSJ4 : 20 cm

Photo 2. Sediment distribution over the floodplain vegetated with model jute plants in the exp. EBSJ.

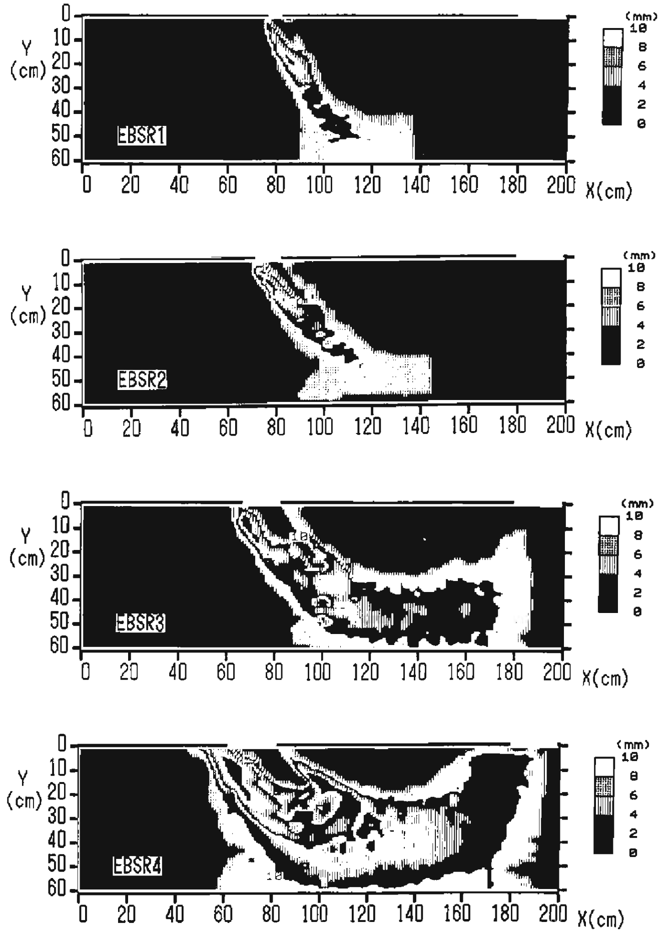

Fig. 3. Sediment distribution patterns in the floodplain vegetated with model rice plants.

downstream water of the floodplain was not turbid, suspending less sediment.

The ratio of the sedimentation volume (V_{sbc}) beyond any corresponding contour line to the total sediment volume (V_{sd}) are expressed as a percentage, V_{sbc}/V_{sd}, and that of the sedimentation area (A_{sbc}) beyond any corresponding contour line to total sediment volume (A_{sd}) are expressed as a percentage, A_{sbc}/A_{sd}. The relations between V_{sbc}/V_{sd}, A_{sbc}/A_{sd} and the dividing contour line (Z_{sl}) are presented in **Fig. 5**. The figure confirms that V_{sbc}/V_{sd} and A_{sbc}/A_{sd} attained 100% earlier in most of EBSR when the Z_{sl} was only around 22 mm, while only about 50% was attained in EBSJ when the Z_{sl} was 22 mm. The ratios, V_{sbc}/V_{sd} and A_{sbc}/A_{sd} attained 100% at a later stage in most of EBSJ when the Z_{sl} was around 35 mm and was limited by the water depth. The ratios indicate some configurations such as degree of concentrated deposition in the confines of the field near a breach. Thus, vegetation would affect the sediment volume and thickness through its roughness effect. Less sedimentation both in volume and thickness was observed to be deposited until the height of vegetation, H_v, was reached, but then increased sharply

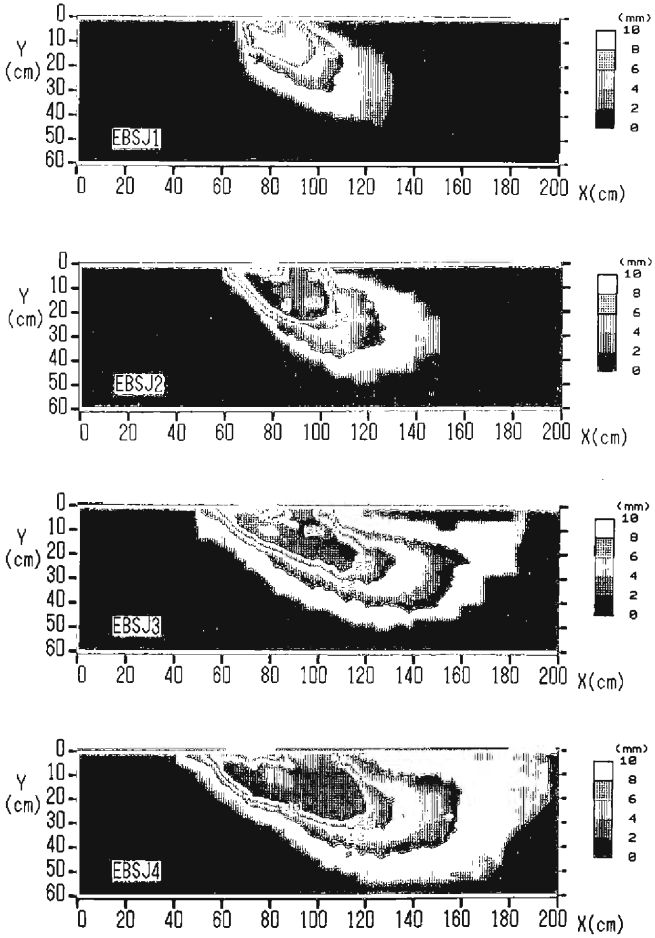

Fig. 4. Sediment distribution patterns in the floodplain vegetated with model jute plants.

after the height of 5.5 mm and the thickness of 25 mm was exceeded for rice and jute plants in EBSR and EBSJ.

3.2 Effect of breach length on floodplain sedimentation

In the experiments, the downstream end of the embankment breach was fixed at the location of x=80 cm, and the upstream end of the breach was shifted upwards at different locations of x=75, 70, 65, and 60 cm to form the embankment breaches of 5, 10, 15, and 20 cm, respectively.

Scouring holes just beyond the breach were seen especially in EBSR. **Fig. 6** shows the relations between the breach lengths (L_b) in the embankment and the scour lengths (L_s) and widths (W_s) for EBSR. The L_s and W_s of the scouring holes just beyond the breaches in the land-side were found to increase with the increase of L_b in the embankments.

On the upstream and downstream sides of a scouring, there were two sediment

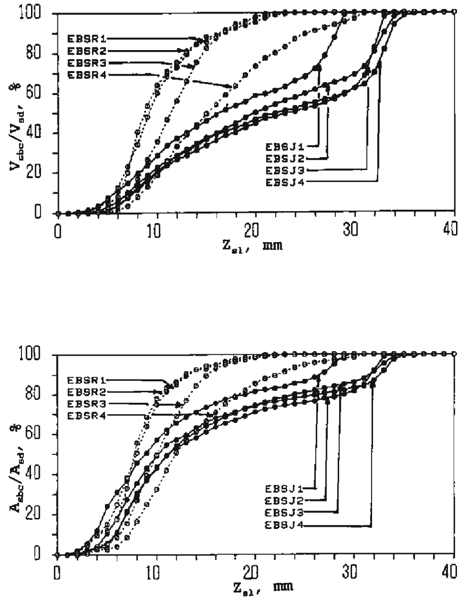

Fig. 5. Relations between V_{sbc}/V_{sd}, A_{sbc}/A_{sd} and Z_{sl}.

ridges with the upstream one being well developed. The sediment thickness in the upper reaches was observed to be higher than ones in the successive lower reaches.

Sediment thickness in the main deposition portion just beyond the embankment breach was observed to be limited up to d_w and did not take place further with the increase of L_b, while new development in sedimentation was observed in the upstream ridge as well as in the lower reaches of downstream with the increase of L_b. The breach length changed the net inflow discharges of water and sediment, the effect being similar to that of elapsed time, which will be discussed in the next chapter.

3.3 Profile, volume and thickness of sedimentation

The sediment deposition height was found to be higher at the upstream portion within x=60 to 120 cm, then gradually decreased towards downstream. The lateral maximum thickness of sediment deposition (Z_{max}) along x is presented in **Table 2** and **Fig. 7**. In the figure, formation of the main deposition with flat top is clear in EBSJ

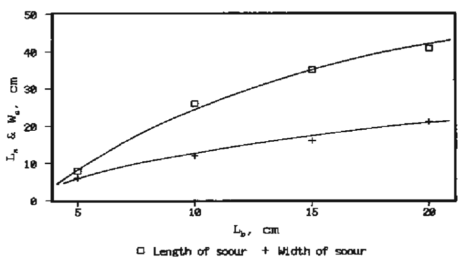

Fig. 6. Relation between L_s, W_s and L_b in the experiments EBSR.

rather than in EBSR. The Z_{max} was observed to be the highest in EBSR4, and was 32.6 mm at x=70 cm, y=7 cm and were followed by EBSR3, EBSR2 and EBSR1. For EBSJ, Z_{max} also did not exceed d_w of 3.6 cm except in EBSJ4, where the highest Z_{max} was found to be 37.8 mm at x=88 cm, y=1 cm. This was because of channel formation on the flat part of the main deposition near the breach.

The laterally averaged thickness of sediment deposition (Z_{ml}) along x is shown in **Fig. 8**. The Z_{ml} was observed to be the highest in EBSR4 and EBSJ4, 18.7 and 25.6 mm, respectively. Mean sediment thickness (Z_{sm}) and the net volumes of total sediment depositions (V_{sd}) over the floodplain for EBSR and EBSJ are shown in **Table 2** and **Fig. 9**. The highest Z_{sm} was observed to be 13.24 mm in EBSR4 and 14.53 mm in EBSJ4. The maximum V_{sd} were 9,200 cm^3 and 7,942 cm^3 in EBSR4 and EBSJ4, respectively. The results of analysis revealed the common trend of sediment deposition, wherein Z_{sm} and V_{sd} over the floodplain increased with the increase of L_b.

Table 2. Z_{max}, Z_{sm} and V_{sd} over the floodplain

Run	Experiment	Z_{max} (mm)	Z_{sm} (mm)	V_{sd} (cm^3)
1	EBSR1	22.1	8.57	1,359
2	EBSR2	23.1	8.61	1,560
3	EBSR3	23.6	10.70	4,469
4	EBSR4	32.6	13.24	9,200
5	EBSJ1	29.0	11.32	1,980
6	EBSJ2	33.5	15.48	3,749
7	EBSJ3	34.4	14.01	6,074
8	EBSJ4	37.8	14.53	7,942

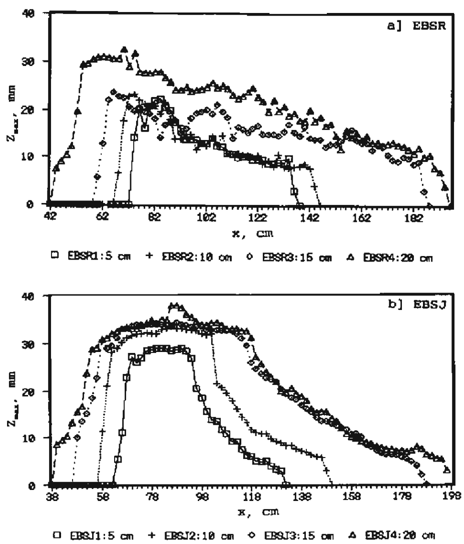

Fig. 7. Z_{max} along x in the experiments EBSR and EBSJ.

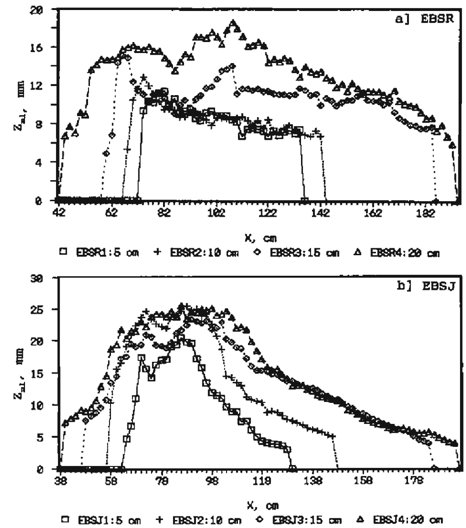

Fig. 8. Z_{ml} along x in the experiments EBSR and EBSJ.

The relations between the volume of total sediment inflow (V_{si}) into the floodplain and the volume of total sediment deposition (V_{sd}) over the floodplain in the model are presented in **Fig. 10**. Considering the fact that the constant river velocity was used instead of the net inflow velocity into the floodplain to estimate V_{si}, the trap efficiency of sediment in the jute plants is rather high. The V_{sd} in both EBSR and EBSJ were observed to increase with the increase of V_{si}. The comparison between EBSR and EBSJ shows that sediment distribution patterns greatly vary according to the different vegeta-

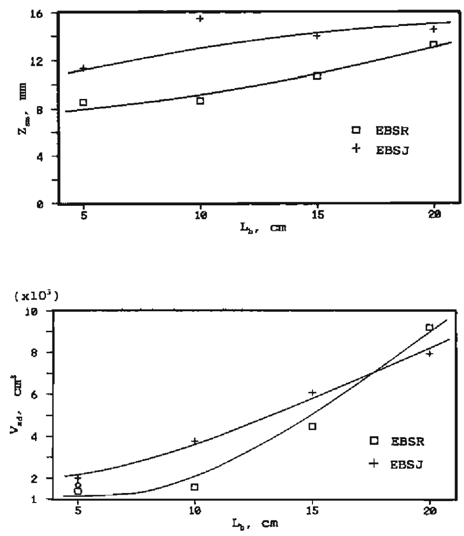

Fig. 9. Relation between Z_{sm}, V_{sd} and L_b over the floodplain.

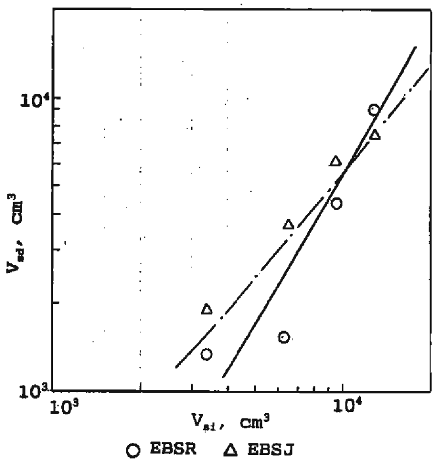

Fig. 10. Relation between V_{sd} and V_{si} in the floodplain.

tion involved. The efficiency of sediment deposition or trap rate as a whole as seen in **Fig. 10** reveals that jute plants are more effective than rice plants in sediment deposition over the floodplain.

After the completion of the former part of the experiments lasting 20 minutes, the experiments were continued for 60 minutes more. Results in this latter part showed that the sediment deposition took place up to a definite limit of maximum thickness and was equal to or less than the d_w in the floodplain as inflow discharge through the floodplain reduced significantly due to the formation of a sediment deposition barrier in the flow. However, sediment deposition in volume and size was found to increase gradually over the floodplain in the latter part of the experiments than those in the former part, as T_e increased.

4. Process of the Floodplain Sedimentation

4.1 Time evolution

To observe further the sediment deposition process over the floodplain due to an embankment breach of 10 cm, the further experiments, EBSR2.TD1, TD2 and TD3 and EBSJ2.TD1, TD2 and TD3, were carried out with durations of 20, 40 and 100 minutes. Perspective views and evolution of patterns of the sedimentation process in EBSR2.TD and EBSJ2.TD are shown in **Photos 3** and **4** and **Figs. 11** and **12**. In EBSR2.TD, after 20 minutes, the deposited portion with the sharp edge similar to that in EBSJ experiment, was established immediately beyond the breach. This is clearly seen in **Photo 3**.

A comparison of the transverse deposition, $Z_{sl.tdp}$ and $Z_{sl.td}$ at x=80 and 94 cm in EBSJ2.TDP, EBSJ3.TDP and EBSJ2.TD is shown in **Fig. 13**. TDP in the figures means that a point gauge was used in the experiments instead of the laser beam gauge. The figure shows that the initial configuration of sedimentation was formed within

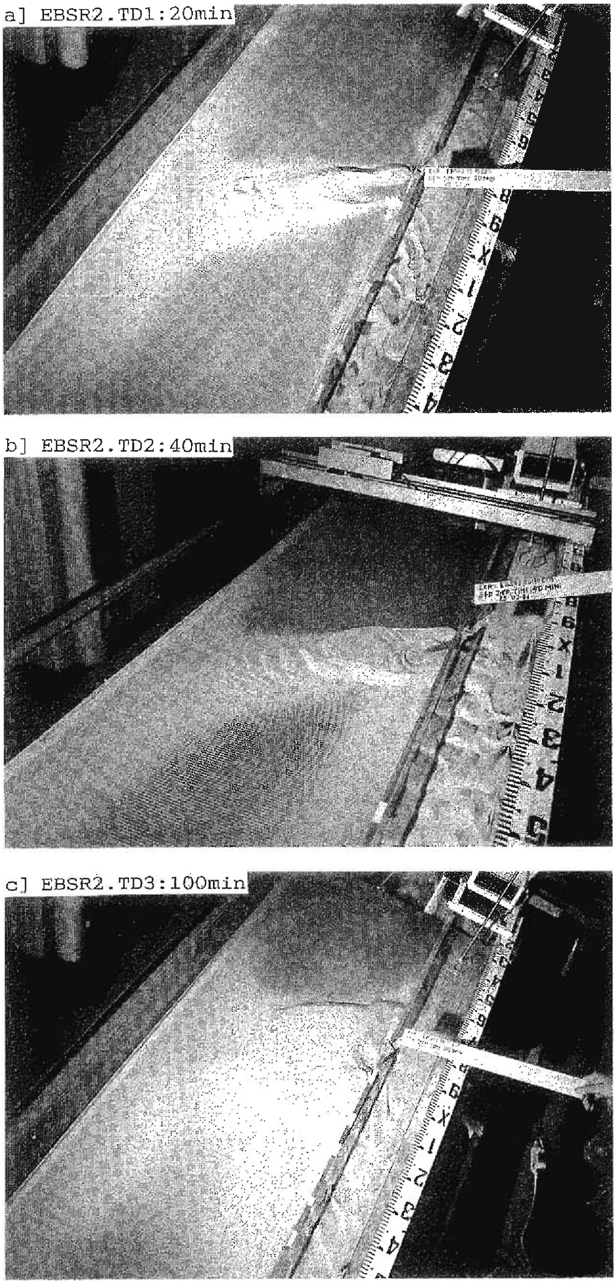

Photo 3. Time dependent sediment distribution over the rice-vegetated floodplain due to embankment breach.

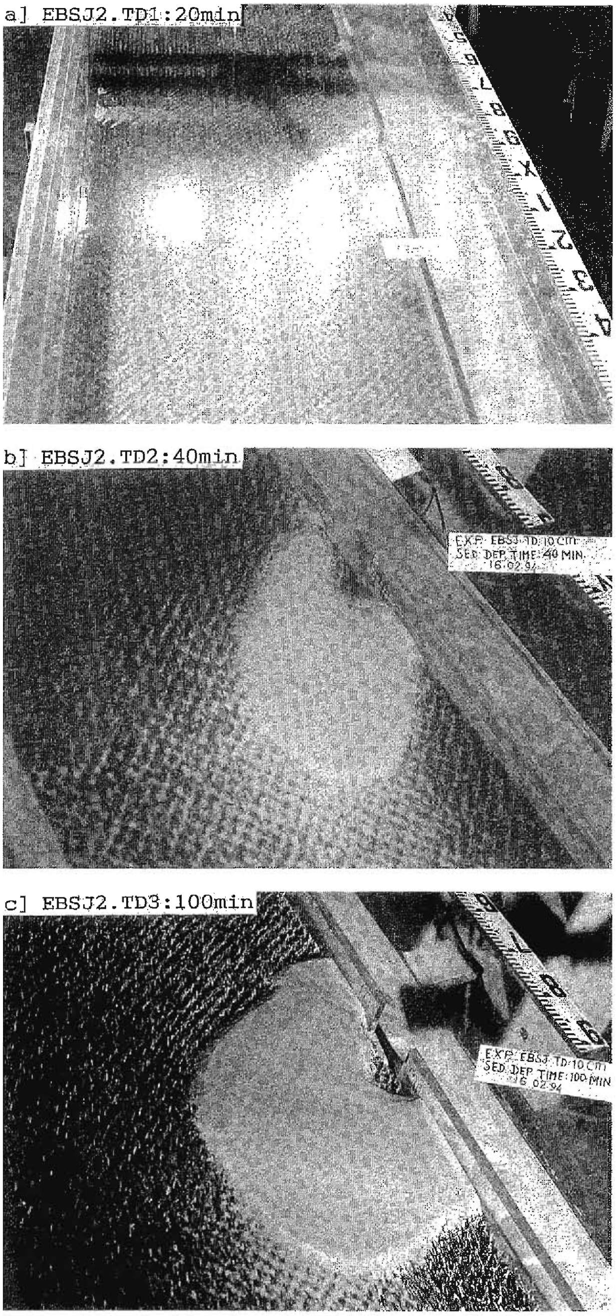

Photo 4. Time dependent sediment distribution over the jute-vegetated floodplain due to embankment breach.

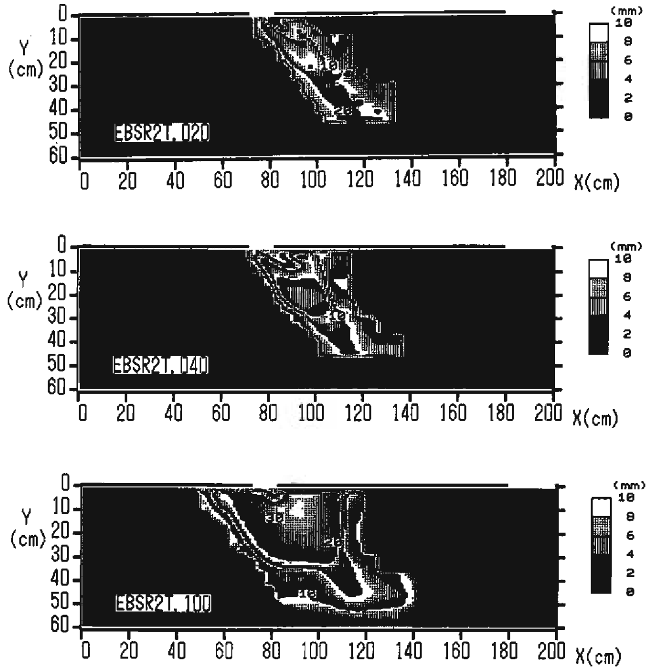

Fig. 11. Time dependent sediment distribution patterns over the rice-vegetated floodplain due to embankment breach.

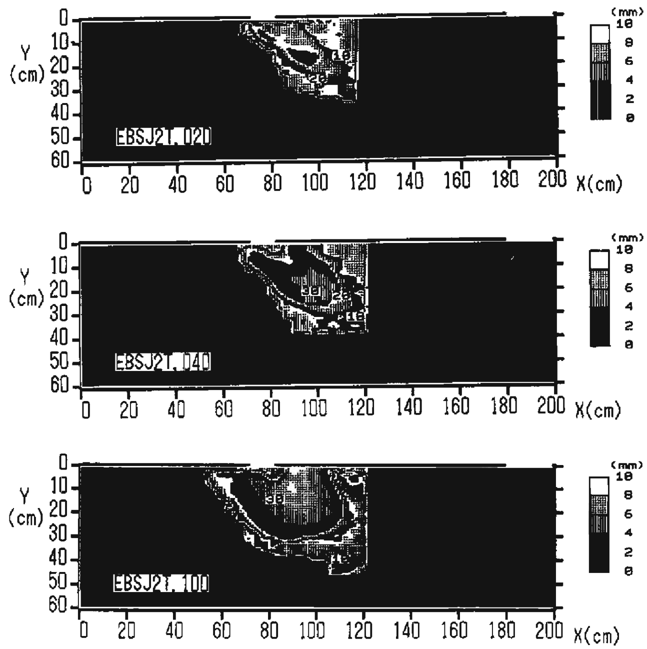

Fig. 12. Time dependent sediment distribution patterns over the jute-vegetated floodplain due to embankment breach.

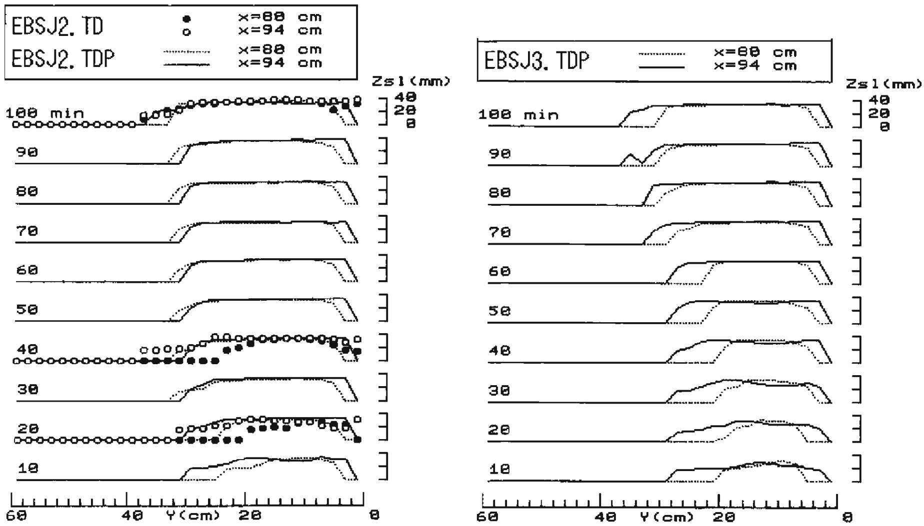

(a) (b)

Fig. 13. $Z_{sl.tdp}$ and $Z_{sl.td}$ along y at x=80 and 94 cm.

10–20 minutes and after that a gradual increase was observed in thickness. In EBSJ3.TDP, newly developed, remarkable sedimentation zone and increase in volume and area was observed with longer times. This process was similar to those of the length dependent basic experiments, EBSJ in runs 5–8.

The thickness of lateral maximum sediment depositions ($Z_{max.td}$) along x for EBSR2.TD and EBSJ2.TD is presented in **Fig. 14**. The highest $Z_{max.td}$ as shown

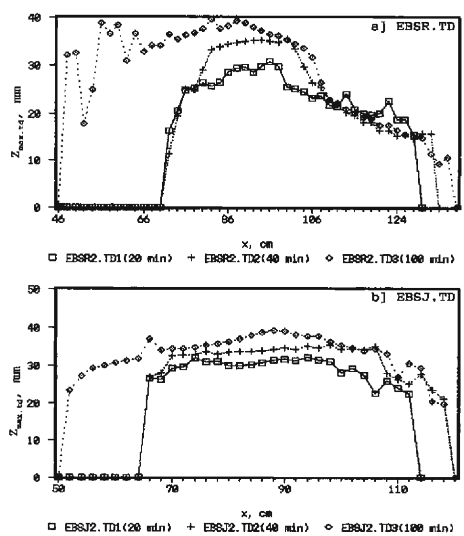

Fig. 14. $Z_{max.td}$ along x in the experiments EBSR.TD and EBSJ.TD.

Table 3. $Z_{max.td}$, $v_{sl.td}$, $Z_{sm.td}$ and $V_{sd.td}$ over the floodplain

Run	Experiment	Time (min)	$Z_{max.td}$ (mm)	$v_{sl.td}$ (cm^2)	$Z_{sm.td}$ (mm)	$V_{sd.td}$ (cm^3)
11	EBSR2.TD1	20	30.7	72.8	18.42	2,610
12	EBSR2.TD2	40	35.6	110.9	16.80	3,180
13	EBSR2.TD3	100	39.4	137.5	19.17	6,738
14	EBSJ2.TD1	20	32.2	79.2	21.83	2,312
15	EBSJ2.TD2	40	35.7	109.9	25.23	3,628
16	EBSJ2.TD3	100	39.5	124.0	25.81	5,216

in **Table 3** was observed to be 39.4 mm in EBSR2.TD3 and 39.5 mm in EBSJ2.TD3 in 100 minutes. These points were made in relation to the fore-mentioned fine channel formation on the major deposition, which made sediment transport outside the channels inactive and left some flat bars or islands. The increase of $Z_{max.td}$ at 100 minutes in comparison to 40 minutes was 10.7% in EBSR2.TD and 10.6% in EBSJ2.TD.

The laterally integrated sediment volume per unit longitudinal length ($v_{sl.td}$) along x for EBSR2.TD and EBSJ2.TD are shown in **Fig. 15**. The highest $v_{sl.td}$ shown in **Table 3** were 137.5 cm^2 in EBSR2.TD3 and 124.1 cm^2 in EBSJ2.TD3 at 100 minutes. The ratio of $v_{sl.td}$ at 100 min to those at 20 min in EBSR2.TD and EBSJ2.TD are 88.9% and 56.6%.

The mean thickness ($Z_{sm.td}$) and net volume ($V_{sd.td}$) of total sediment deposition over the floodplain for EBSR2.TD and EBSJ2.TD are presented in **Table 3** and **Fig. 16**. The increase of $Z_{sm.td}$ at 100 minutes in comparison to 20 minutes was negligible in EBSR2.TD and 18.2% in EBSJ2.TD. The net volume increased significantly at 100 minutes in comparison to that at 20 minutes by 158.2% in EBSR2.TD and 125.6% in

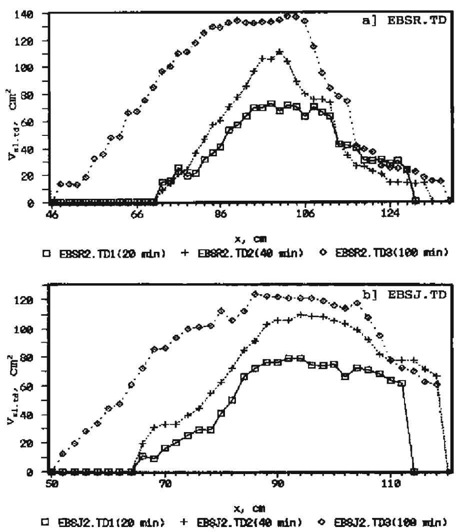

Fig. 15. $v_{sl.td}$ along x in the experiments EBSR2.TD and EBSJ2.TD.

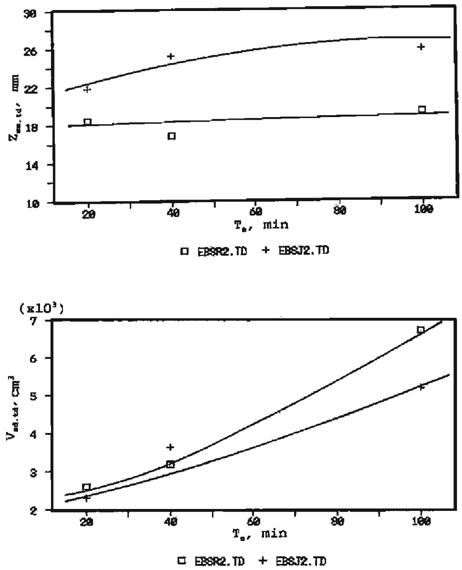

Fig. 16. Relations between $Z_{sm.td}$, $V_{sd.td}$ and T_e.

EBSJ2.TD.

Using the advective time ratio of 100, the time duration of 20 minutes in the experiment corresponds to 33 hours in the field, which is within a possible range, and the experiment covers long enough time span.

4.2 Effect of river discharge

To observe the discharge dependent sediment distribution process over the floodplain due to an embankment breach of 20 cm, EBSJ4.DD1, DD2 and DD3 were carried out for 20 minutes each with a river discharge of 1,080 cm^3/s, 1,620 cm^3/s and 2,160 cm^3/s, respectively. Perspective views and their patterns over the floodplain in EBSJ4.DD are shown in **Photo 5** and **Fig. 17**. Sediment thickness was observed to be higher than 30 mm just beyond the breach. The difference between DD3 and DD2 in the upper portion was small, while that between DD2 and DD1 was remarkable.

The thickness of longitudinal sediment distributions ($Z_{sln.dd}$) at each different x was found to be higher at the upstream within around x=60–100 cm and gradually decreased towards downstream within the sediment deposited area. The maximum sediment deposition was observed to be almost equal to or less than the d_w of 36 mm.

The lateral maximum thickness ($Z_{max.dd}$) for EBSJ4.DD is shown in **Table 4** and **Fig. 18**, which shows the typical shape with the flat top for the case of DD3, and the highest $Z_{max.dd}$ was 36.0 mm. The increase in $Z_{max.dd}$ in DD3 was found to be 4.3% and 14.3% in comparison to those of DD2 and DD1, respectively. The sediment volume per unit longitudinal length ($v_{sl.dd}$) for EBSJ4.DD is shown in **Table 4** and **Fig. 19**. The $v_{sl.dd}$ was observed to be the highest and increased significantly in DD3 by 28.1% and 75.0%, compared to those of DD2 and DD1, respectively. The figure shows increasing

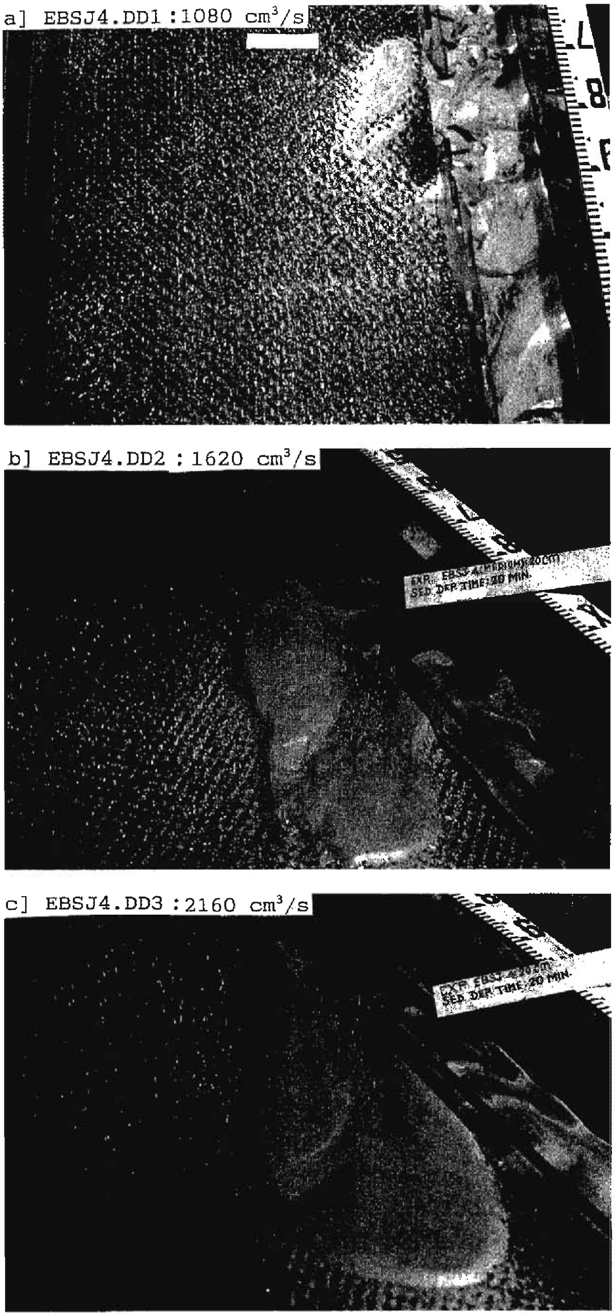

Photo 5. Discharge dependent sediment distribution over the jute-vegetated floodplain due to embankment breach.

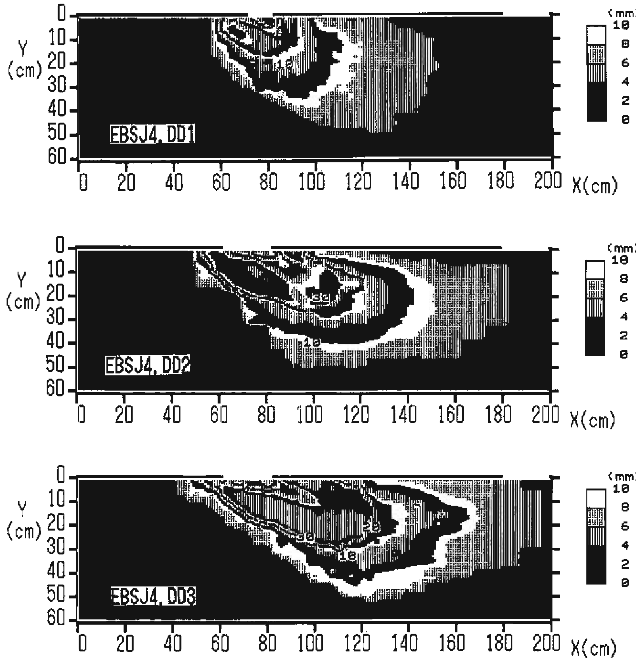

Fig. 17. Discharge dependent sediment distribution patterns over the jute-vegetated floodplain due to embankment breach.

Table 4. $Z_{max.dd}$, $v_{sl.dd}$, $Z_{sm.dd}$ and $V_{sd.dd}$ over the floodplain

Run	Experiment	Discharge (cm^3/s)	$Z_{max.dd}$ (mm)	$v_{sl.dd}$ (cm^2)	$Z_{sm.dd}$ (mm)	$V_{sd.dd}$ (cm^3)
17	ESJ4.DD1	1,080	31.5	68.8	9.72	3,273
18	EBSJ4.DD2	1,620	34.5	94.0	13.69	6,045
19	EBSJ4.DD3	2,160	36.0	120.4	14.46	7,462

development towards downstream.

The mean thickness ($Z_{sm.dd}$) and total sediment volume ($V_{sd.dd}$) of depositions over the floodplain for EBSJ4.DD are presented in **Fig. 20.** A little increase in $Z_{sm.dd}$ was

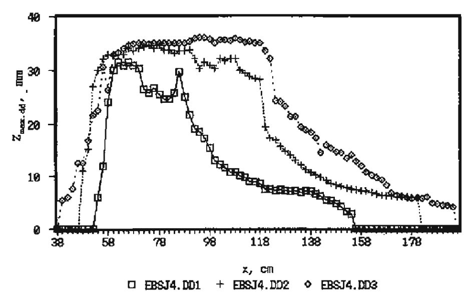

Fig. 18. $Z_{max.dd}$ along x in the experiments EBSJ4.DD.

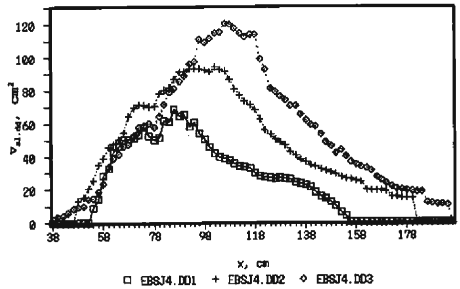

Fig. 19. $v_{sl.dd}$ along x in the experiments EBSJ4.DD.

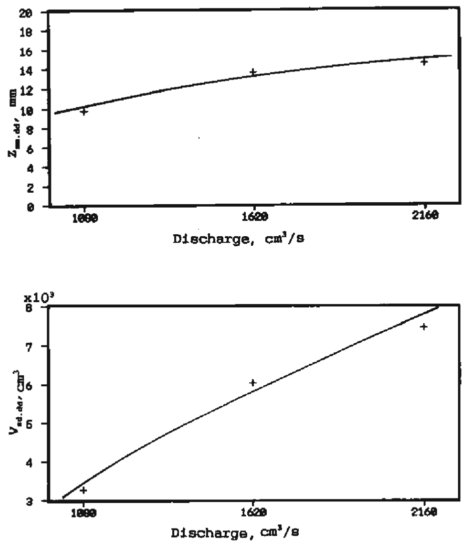

Fig. 20. Relations between $Z_{sm.dd}$, $V_{sd.dd}$ and different discharges.

observed in DD3 in comparison to those of DD2 and DD1, while $V_{sd.dd}$ increased significantly in DD3 by 128.0% in comparison to that of DD1. These characteristics will serve as reference to the sedimentation process during the rising stage of the flood with increasing discharge.

5. Conclusion

Based on the above discussion on the results of the model experiments the following conclusions are drawn:

(1) The sediment deposition over the floodplain due to the embankment breach increased in volume (V_{sd} and v_{sl}) and thickness (Z_{sl} and Z_{sm}) with the increase of the breach length (L_b) in the failure embankments.

(2) Sediment deposition process over the floodplain can broadly be divided into two stages: i) formation of initial configuration and maximum thickness of sediment deposi-

tion upto a definite limit not exceeding the water depth in the floodplain at the main portion of deposition just after the breach attained in around 20 minutes; ii) gradual lateral and longitudinal development of sedimentation in new area over the floodplain extending more towards the upstream. At this moment remarkable increase in sedimentation volume and area were observed with the duration of elapsed time. With the fixed downstream edge of embankment breach, formation of sharp ridges in sedimentation are observed upstream of the deposited area with the shifting of the upstream edge of the embankment breach to upstream.

(3) The sediment thickness (Z_{sl}, Z_{max}, Z_{ml} and Z_{sm}) and volume (v_{sl} and V_{sd}) are observed to be higher over the floodplain with the model jute plants in the experiments EBSJ in runs 5–8 than those with the rice plants in the experiments EBSR in runs 1–4. Vegetation resistance plays an effective and important role on the sedimentation over the floodplain. Sedimentation both in volume and thickness was observed to be less over the floodplain until it exceeded the vegetation height (H_v) and increased sharply after exceeding H_v. No difference was observed in the final stage of sedimentation over the floodplain irrespective of the different vegetation at the main portion of deposition immediately beyond the breach in the embankment.

(4) In the time dependent experiments, EBSR2.TD and EBSJ2.TD in runs 11–16, the sediment thickness ($Z_{sl.td}$, $Z_{max.td}$, $Z_{ml.td}$ and $Z_{sm.td}$) was attained in 20–40 minutes, increasing negligibly even in 100 minutes, while volume ($v_{sl.td}$ and $V_{sd.td}$) and area of the sediment deposition increased significantly in 100 minutes in comparison to those of 20–40 minutes. Though the initial sedimentation depended on the H_v, the final volume and area of sedimentation depended on long term deposition time elapsed.

(5) In the discharge dependent experiments, EBSJ4.DD in runs 17–19, the sediment thickness ($Z_{max.dd}$, $Z_{ml.dd}$ and $Z_{sm.dd}$) over the floodplain did not increase remarkably, but volume ($v_{sl.dd}$ and $V_{sd.dd}$) and size of the sediment deposition increased significantly with the increase of the discharge in the river channel.

(6) The time and discharge dependent sedimentation processes observed in EBSR2.TD, EBSJ2.TD and EBSJ4.DD, were similar to those of the length dependent basic experiments of EBSR and EBSJ in runs 1–8. The sediment deposition process over the floodplain due to the embankment breach depended upon the volume of sediment inflow (V_{si}) into the floodplain mainly composed of five hydraulic parameters: water depth in the floodplain, breach length in the embankment, sediment concentration in river water, discharge in the river channel, and duration of elapsed time.

Acknowledgement

The study was conducted under the financial support of the Japan Society for the Promotion of Science (JSPS) in the form of a fellowship to the first author which is gratefully acknowledged.

REFERENCES

1) Ahmed, S. M. U., M. M. Hoque and S. Hossain (1992): Floods in Bangladesh: A Hydrological Analysis, Final Report R01/92, Institute of Flood Control and Drainage Research (IFCDR), Bangladesh University of Engineering and Technology(BUET), Dhaka, pp. 1–5.
2) Bangladesh Water Development Board: Flood in Bangladesh (1987): Investigation, Review and Recommendations for Flood Control, Dhaka, pp. 31–39.
3) Choudhury, A. M. (1990): Use of Remote Sensing Techniques in Flood Study, Flood Study Forum 1990, 'Floods in Bangladesh: Bangladesh Views', Dhaka, pp. 7–13.
4) Coleman, J. M. (1969): Brahmaputra River: Channel Processes and Sedimentation, Sedimentary Geology, vol. 3, Amsterdam, pp. 29–141.
5) Hoque, M. M., S. M. U. Ahmed and A. B. Siddique (1991): Effects of Different Planning Options on Floods in Bangladesh: A Numerical Model Study, Partial Completion Report, R04/91, IFCDR, BUET, Dhaka, pp. 1–5.
6) Islam, M. Z. (1991): Failure of Flood Embankments: Case Studies of Some Selected Projects in Bangladesh, IFCDR, BUET, Dhaka, pp. 1–160.
7) Klaassen G. J., K. Vermeer and U. Nazim (1988): Sedimentological processes in the Jamuna River, Bangladesh, Proceedings of the International Conference on Fluvial Hydraulics, Budapest, pp. 1–2.
8) Muramoto, Y., Y. Fujita and K. Okubo (1989): Floodplain Erosion and Sedimentation due to Overbank Flood Flow, Proceedings of the Japan-China (Taipei) Joint Seminar on Natural Hazard Mitigation, Kyoto, pp. 429–438.
9) Nakagawa, H., T. Takahashi and M. Higashiyama (1989): Suspended Sediment Deposition in Flood Plains due to Meandering River Bank Breach, Proceedings of the Fourth International Symposium on River Sedimentation, Beijing, pp. 587–595.
10) Pramanik, M. A. H. (1993): Floods and Cyclones Disasters in Bangladesh, Seisan-Kenkyu, Vol. 45, No. 3, Inst. of Industrial Science, Univ. of Tokyo, pp. 177–184.
11) Shieh C. L. (1989): A study on the Delta Formation Process in a Laterally Wide Basin, Ph. D. thesis, Department of Civil Engineering, Kyoto University, Kyoto, pp. 10–13.
12) Takahashi, T., H . Nakagawa and M. Higashiyama (1988): Sedimentation in Flood Plains due to River Bank Breach, Proceedings of the 6th Congress, Asian and Pacific Regional Division, International Association for Hydraulic Research, Kyoto, pp. 401–408.